Available online at www.sciencedirect.com
SCIENCE DIRECT®
Journal of Power Sources 115 (2003) 110–118
JOURNAL OF POWER SOURCES
www.elsevier.com/locate/jpowsour

$LiMn_2O_4$ cathode doped with excess lithium and synthesized by co-precipitation for Li-ion batteries

H.W. Chan[a], J.G. Duh[a,*], S.R. Sheen[b]

[a]*Department of Materials Science and Engineering, National Tsing Hua University, Hsinchu, Taiwan*
[b]*Coremax Taiwan Corporation, Hsinchu Hsien, Taiwan*

Received 20 August 2002; accepted 9 November 2002

Abstract

$LiMn_2O_4$ exhibits lower cost, acceptable environmental characteristics, and better safety properties than other positive-electrode (cathode) materials for lithium-ion batteries. In this study, excess Li doped $Li_{1+x}Mn_2O_4$ is synthesized by a well-mixed co-precipitation method with LiOH utilized as both the reactant and co-precipitation agent. The precursor is calcined for various heating times and temperatures to form a fine powder of a single spinel phase with different particle sizes, size distributions, and morphology. The minimum heating temperature is around 400 °C. For short heating periods, Mn_2O_3 impurity is observed, but disappears after longer heating times. The average particle size is in the range 2–8 μm for powders calcined between 700 and 870 °C. The lattice parameter increases with increase in heating temperature. The electrochemical behavior of $LiMn_2O_4$ powder is examined by using test cells which consist of a cathode, a metallic lithium anode, and an electrolyte of 1 M $LiPF_6$ in a 1:1 (volume ratio) mixture of ethylene carbonate (EC) and dimethyl carbonate (DMC). Cells with cathodes of $LiMn_2O_4$, $Li_{1.08}Mn_2O_4$ and $Li_{1.1}Mn_2O_4$ give a capacity of 85, 109 and 126 mAh g^{-1}, respectively. The introduction of excess Li in $LiMn_2O_4$ apparently increases the capacity, and decreases significantly the rate of capacity degradation on charge–discharge cycling.

Keywords: Lithium-ion battery; Cathode material; Co-precipitation method; Excess lithium; $LiMn_2O_4$; Capacity

1. Introduction

The positive-electrode (cathode) material plays a critical role in the performance of Li-ion batteries. Accordingly, various kinds of cathode materials of low material cost, high stability and good electrochemical performance have been investigated. Some of candidates are $LiMn_2O_4$ with a spinel (*Fd3m*) structure, $LiCoO_2$ and $LiNiO_2$ with layer (*R3m*) structure, and $LiNiVO_4$ and $LiCoVO_4$ [1] with an inverse spinel (*Fd3m*) structure.

The ternary lithium manganese oxide, $LiMn_2O_4$, and its related compounds have been studied extensively as a cathode material with three-dimensional framework for Li-ion rechargeable cells. $LiMn_2O_4$ was first synthesized is 1958 [2] by heating a mixture of lithium carbonate and manganese oxide at 850 °C in air. In 1981, Hunter [3] reported that lithium ions could be de-intercalated completely from the spinel $LiMn_2O_4$ structure to form λ-MnO_2 by a chemical procedure [3]. Given this performance, Thackeray et al. used $LiMn_2O_4$ as a cathode material in 1983 [4]. The theoretical specific capacity of $LiMn_2O_4$ is 148 mAh g^{-1}, and the practical specific capacity approaches 120 mAh g^{-1}. For some applications, however, a capacity of about 120 mAh g^{-1} is acceptable, provided the value remains stable under extended charge–discharge cycling. During de-intercalation, lithium ions leave the spinel $LiMn_2O_4$ structure and this leads to the formation of Mn_2O_4 in which the spinel structure is retained. It is supposed that lithium ions can be intercalated fully from the host structure and that the structure does not deteriorate as do $LiNiO_2$ and $LiCoO_2$ when lithium ions are extracted.

Spinel $LiMn_2O_4$ is usually synthesized at high temperatures by a solid-state reaction [5]. At lower temperatures, some Mn_2O_3 may be present as an impurity and only disappears at 800 °C [6–8]. Compared with the solid-state method, the stoichiometry of lithium manganese oxide can be controlled more exactly by the co-precipitation method.

In this study, a simple modified approach is adopted to provide $LiMn_2O_4$ with adequate electrochemical properties for use in Li-ion rechargeable batteries. The co-precipitation method is carried out in de-ionized water using LiOH as reactant and a co-precipitation agent. The selection of LiOH decreases the complexity of the co-precipitation method and

* Corresponding author. Fax: +886-3-571-2686.
E-mail address: jgd@mse.nthu.edu.tw (J.G. Duh).

0378-7753/02/$ – see front matter
PII: S0378-7753(02)00616-X

allows a more intimate mixing of lithium and manganese in the starting materials, which results in a homogeneous $LiMn_2O_4$ product with well-controlled morphology. In addition, excess Li^+ ions act as a 'reservoir' to overcome the well-known loss in capacity during the first charge of lithium-ion batteries [9,10].

2. Experimental

2.1. Powder preparation

Stoichiometric, excess-Li, spinel $Li_{1+x}Mn_2O_4$ was synthesized from the reaction of a mixture of lithium hydroxide (LiOH) and manganese acetate ($Mn(CH_3COO)_2$). A stoichiometric amount of the latter two compounds a cationic ratio of Li:Mn $= (1 + x)$:2 was dissolved in deionized water and mixed well by stirring gently. The sample designation is listed in Table 1. The solution was evaporated at 100 °C for 10 h to obtain the precursor powder. The precursor was preheated at 400 °C for 1 h, and then calcined at elevated temperature at a rate of 2 °C/min in air to examine the reaction process for the formation of single-phase $LiMn_2O_4$.

2.2. Characterization and analysis

Thermogravimetry/diffrential thermal analysis (TG/DTA, SSC 5000, Seiko, Japan) was employed to determine the preheating and minimum calcine temperature with the heating rate of 10 °C/min from room temperature to 1000 °C. The compositions of the calcined powder were analyzed with an inductively coupled plasma–atomic emission spectrometer (ICP–AES, Perkin-Elmer, Optima 3000 DV, USA), and were further determined with an electron probe microanalyzer (EPMA, JXA-8800M, JEOL, Japan). Since lithium cannot be detected by EPMA, the contents of manganese and oxygen were first evaluated by means of the ZAF technique in EPMA and then the amount of lithium was obtained by a difference and normalization approach. The phase composition and crystal structure of the heat-treated powder were analyzed with an X-ray diffractometer (XRD) operated at 30 kV and 20 mA from 15 to 70° (Rigaku, D/MAX-B, Japan) with a wavelength of Cu Kα ($\lambda =$ 1.5406 Å). The particle size and distribution of the precursor and spinel $LiMn_2O_4$ powder were examined by laser scattering (Horiba, LA 300, Japan). The particle morphology was observed using a field emission scanning electron microscope (FESEM, JSM-6500F, JEOL, Japan) at an accelerating voltage of 15 kV.

Table 1
Sample designation of $Li_{1+x}Mn_2O_4$ series

Sample designation	Formulation
LMO	$LiMn_2O_4$
$L_{1.02}$MO	$Li_{1.02}Mn_2O_4$
$L_{1.05}$MO	$Li_{1.05}Mn_2O_4$
$L_{1.08}$MO	$Li_{1.08}Mn_2O_4$
$L_{1.1}$MO	$Li_{1.1}Mn_2O_4$

2.3. Electrochemical characterization

The electrochemical behavior of $LiMn_2O_4$ powder was examined by using two-electrode test cells which consisted of a cathode, a metallic lithium anode, a polypropylene

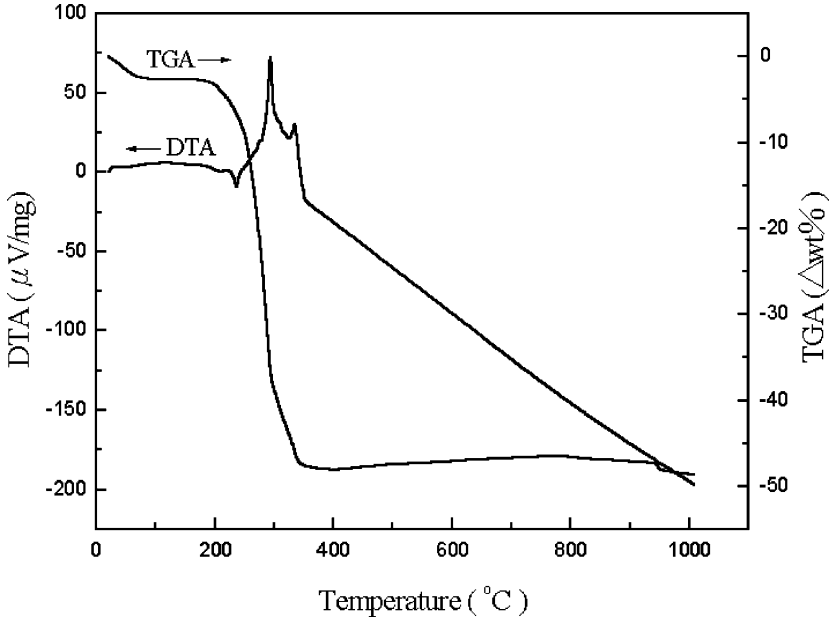

Fig. 1. TG/DTA trace of $Li_{1.08}Mn_2O_4$ precursor heat-treated from room temperature to 1000 °C at the rate of 10 °C/min in air.

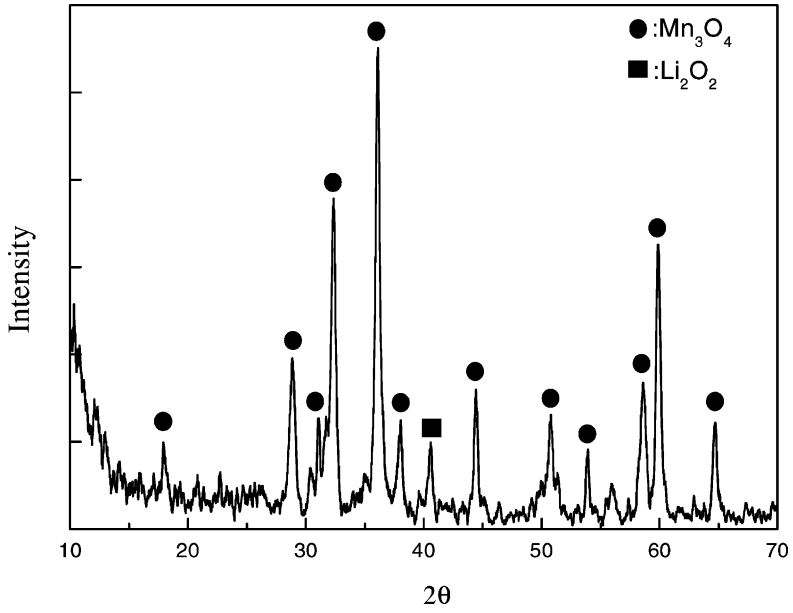

Fig. 2. XRD pattern of $LiMn_2O_4$ precursor heat-treated at 300 °C for 1 h.

separator and an electrolyte of 1 M $LiPF_6$ in a 1:1 (volume ratio) mixture of ethylene carbonate (EC) and dimethyl carbonate (DMC). All procedures in fabricating the cells were carried out in a specially-designed chamber with low oxygen pressure and low moisture. The slurry was made of lithium manganese oxide powders with carbon black and PVDF in the weight ratio of 85:10:5. The cathodes were prepared by casting the slurry on to an aluminum foil, and then drying at 120 °C for 12 h. Cells were cycled within the potential range 3.0–4.2 V at the 0.1*C* rate for the first cycle and then at the 0.2*C* rate for the second cycle, onwards.

3. Results and discussion

3.1. Thermal analysis

In order to determine the chemical reaction of the precursor and the calcining temperature of the co-precipitation products, thermal analysis is necessary to define the optimum heat-treated temperature.

A TG/DTA trace of the decomposition of the precursor for a powder of $Li_{1.08}Mn_2O_4$ at 10 °C/min in air is presented in Fig. 1. The TGA curve can be divided into three regions: (i)

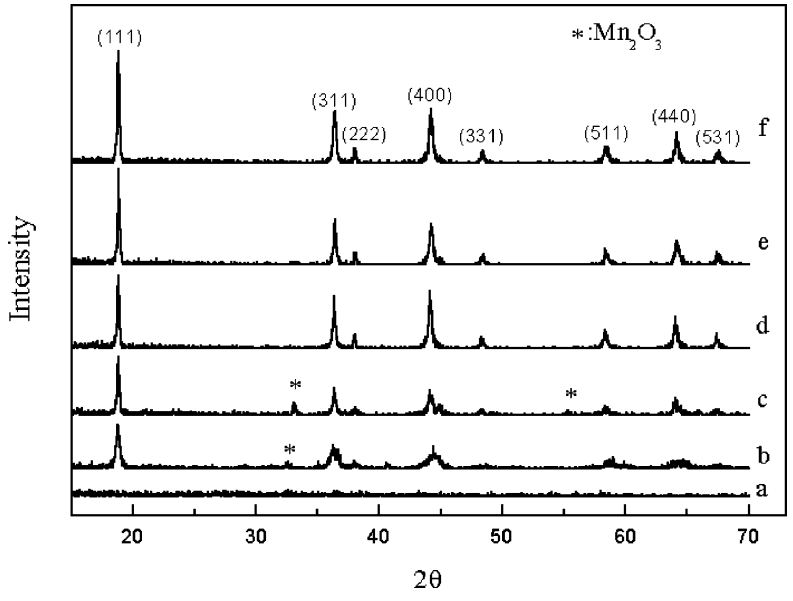

Fig. 3. XRD pattern of $LiMn_2O_4$ precursor heat-treated at various temperatures for 10 h: (a) precursor; (b) 400 °C; (c) 500 °C; (d) 600 °C; (e) 700 °C; (f) 800 °C.

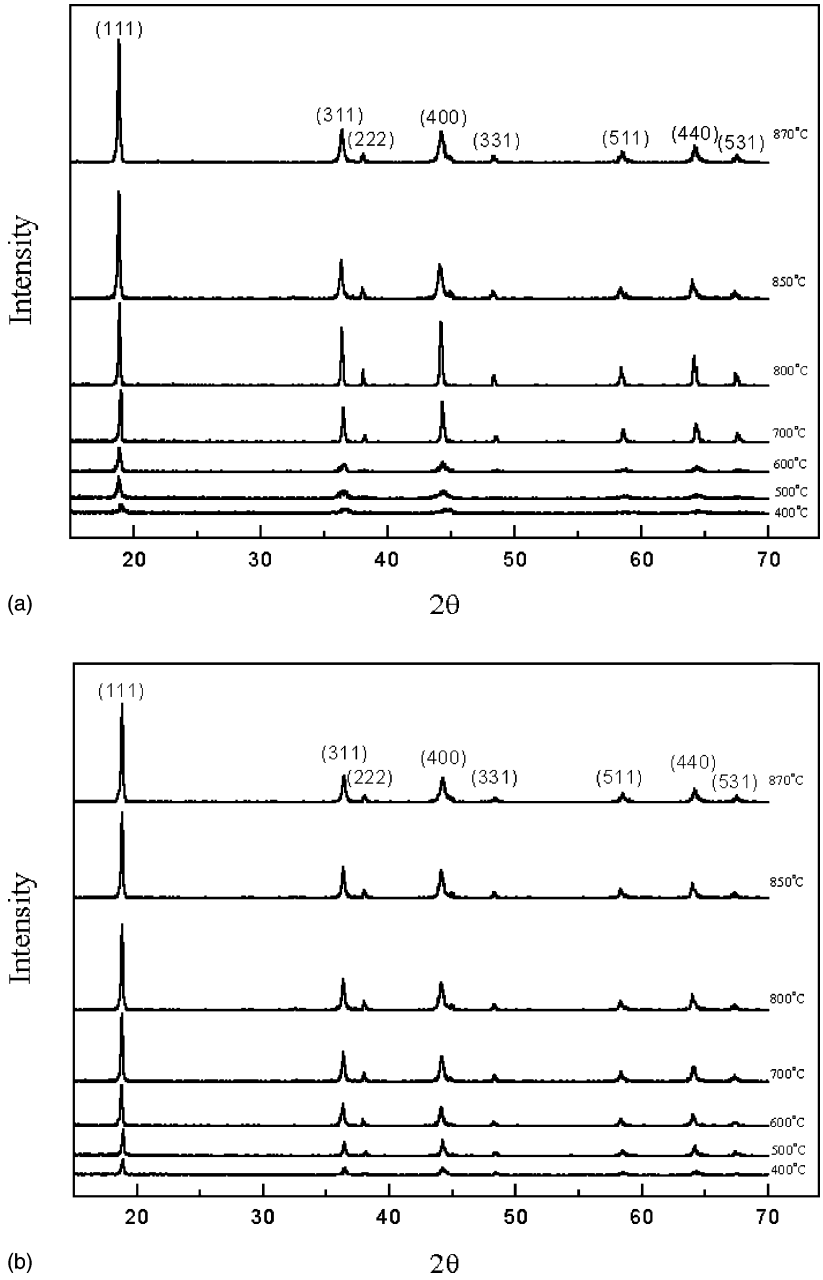

Fig. 4. XRD pattern of (a) $LiMn_2O_4$ and (b) $Li_{1.08}Mn_2O_4$ precursor heat-treated at elevated temperature for 15 h.

an initial weight loss of 5% near 100 °C; (ii) a further weight loss of 35% between 200 and 300 °C; (iii) a final weight loss of 9% that is nearly completed at 350 °C. In addition, the DTA curve of Fig. 1 shows an endothermic peak around 100 °C, which is assigned to the evaporation of free water which has been absorbed from the atmosphere. The endothermic peak around 250 °C can be attributed to hydration in the molecules of Li_2O_2 and Mn_3O_4, which was confirmed by XRD, as shown in Fig. 2. The two large exothermic peaks in the final temperature range between 290 and 330 °C might be due to the decomposition of the residual organics in Li_2O_2 and Mn_3O_4 that then form the spinel phase, $LiMn_2O_4$.

From the TG/DTA trace, the total weight loss of the $Li_{1+x}Mn_2O_4$ precursor is about 50%. Therefore, the lowest temperature of $Li_{1+x}Mn_2O_4$ to form the spinel structure is taken to be 380 °C.

3.2. Phase identification

In order to confirm the phase composition and the crystallinity of the heat-treated powder, analysis by XRD and EPMA is essential.

The co-precipitated precursor was heated at elevated temperatures for its evolution to the final spinel structure. The XRD pattern of the precursor $LiMn_2O_4$ is shown in

Fig. 3a. The data indicate that the as-fabricated precursor is amorphous without crystallinity. At 400 °C for 10 h, there appears some broad diffraction peaks of low intensity, which indicate the incomplete formation of $LiMn_2O_4$. Several minor peaks are also present, which are identified as Mn_2O_3, as shown in Fig. 3b. With increase in temperature, the peak intensity and crystallinity of $LiMn_2O_4$ increases, while the impurity phase Mn_2O_3 disappears. Lithium manganese oxide with well-developed crystallinity is obtained at 800 °C for 10 h (see Fig. 3f). Although the impurity phase Mn_2O_3 is observed in the initial stage, increasing the heat-treated time may be a good way to solve this problem. $LiMn_2O_4$ was further calcined at various temperatures for 15 h as shown in Fig. 4. No impurity phase is observed from 400 to 870 °C and a high crystalline spinel phase at high temperature can be obtained. Thus, it is concluded that an effective way to avoid the formation of the impurity phase of Mn_2O_3 is by raising the heat-treated temperature or by prolonging the sintering time. The broadening of diffraction peaks at high scattered angles is indicative of residual strains [11], which are caused by inhomogeneities, cation or anion non-stoichiometry vacancies, and grain boundary effects in the structure. In fact, the strains can be reduced or removed through an increase in the heat-treatment temperature.

The presence of a $LiMn_2O_4$ major phase with impurity Mn_2O_3 can be detected from a back-scattered electron image (BEI) of the morphology which is obtained by EPMA. For the precursor $LiMn_2O_4$ calcined at 700 °C for 5 h, the impurity phase Mn_2O_3 is observed on the basis of the XRD pattern, as indicated in Fig. 5a. The white aggregation within the grey matrix of the BEI morphology in Fig. 5b corresponds to Mn_2O_3. After a further 5 h of heat-treatment, i.e. for a total period of 10 h, the white aggregation disappears and only a grey matrix is observed. This indicates a more homogeneous phase, as shown in Fig. 5c. Quantitative analysis by EPMA shows that the Mn:O ratio in the white aggregate in Fig. 5b is 2:3, while that in Fig. 5c is 2:4. This provides further evidence that the impurity phase for short-time sintering is Mn_2O_3, but $LiMn_2O_4$ prevails after a long period of time.

Table 2
Phase distribution for $Li_{1+x}Mn_2O_4$ sintered at various temperatures for 5–15 h

Phase identification	Time (h)	Temperature (°C)				
		700	750	800	850	870
LMO	5	MP[a]	MSP[b]	MSP	MP	MP
	10	PSP[c]	PSP	PSP	PSP	PSP
	15	PSP	PSP	PSP	PSP	PSP
$L_{1.02}MO$	5	MP	MP	MSP	MSP	MSP
	10	PSP	PSP	PSP	PSP	PSP
	15	PSP	PSP	PSP	PSP	PSP
$L_{1.05}MO$	5	MSP	MP	PSP	MSP	MSP
	10	PSP	PSP	PSP	PSP	PSP
	15	PSP	PSP	PSP	PSP	PSP
$L_{1.08}MO$	5	PSP	PSP	MP	MSP	PSP
	10	PSP	PSP	PSP	PSP	PSP
	15	PSP	PSP	PSP	PSP	PSP
$L_{1.1}MO$	5	MSP	MSP	MSP	PSP	PSP
	10	PSP	PSP	PSP	PSP	PSP
	15	PSP	PSP	PSP	PSP	PSP

[a] MP: mixed phase of spinel and Mn_2O_3.
[b] MSP: major spinel phase with trace Mn_2O_3 peak visible.
[c] PSP: pure spinel phase without other detectable phase.

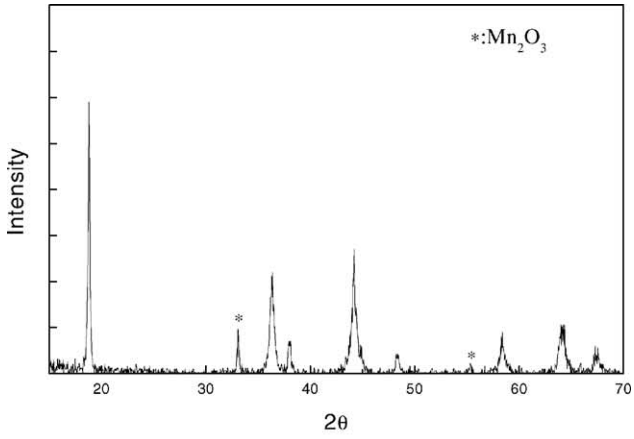

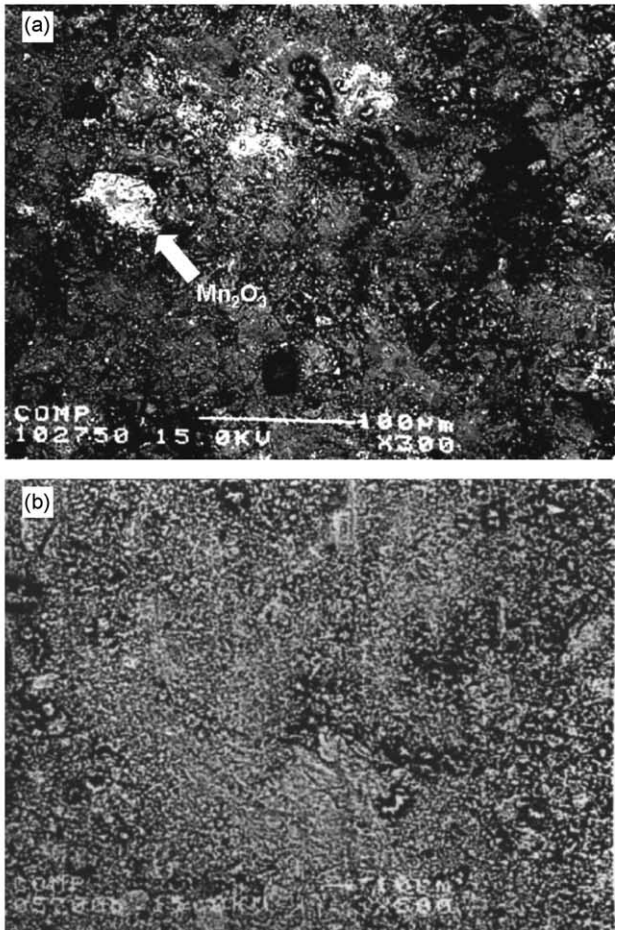

Fig. 5. XRD pattern of (a) $LiMn_2O_4$ calcined at 700 °C for 5 h and BEI morphology of $LiMn_2O_4$ calcined at 700 °C for (b) 5 h and (c) 10 h.

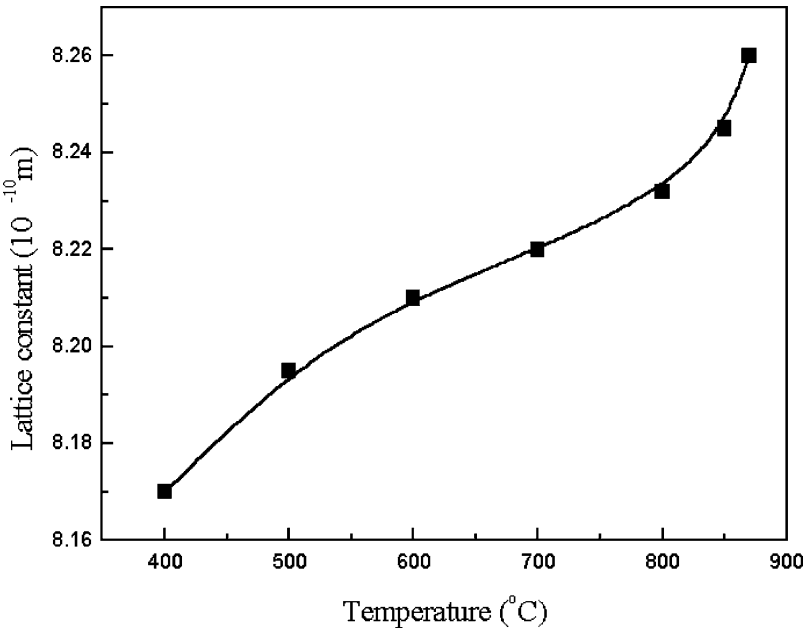

Fig. 6. Lattice constant vs. heat-treated temperature for calcined $LiMn_2O_4$ for 10 h.

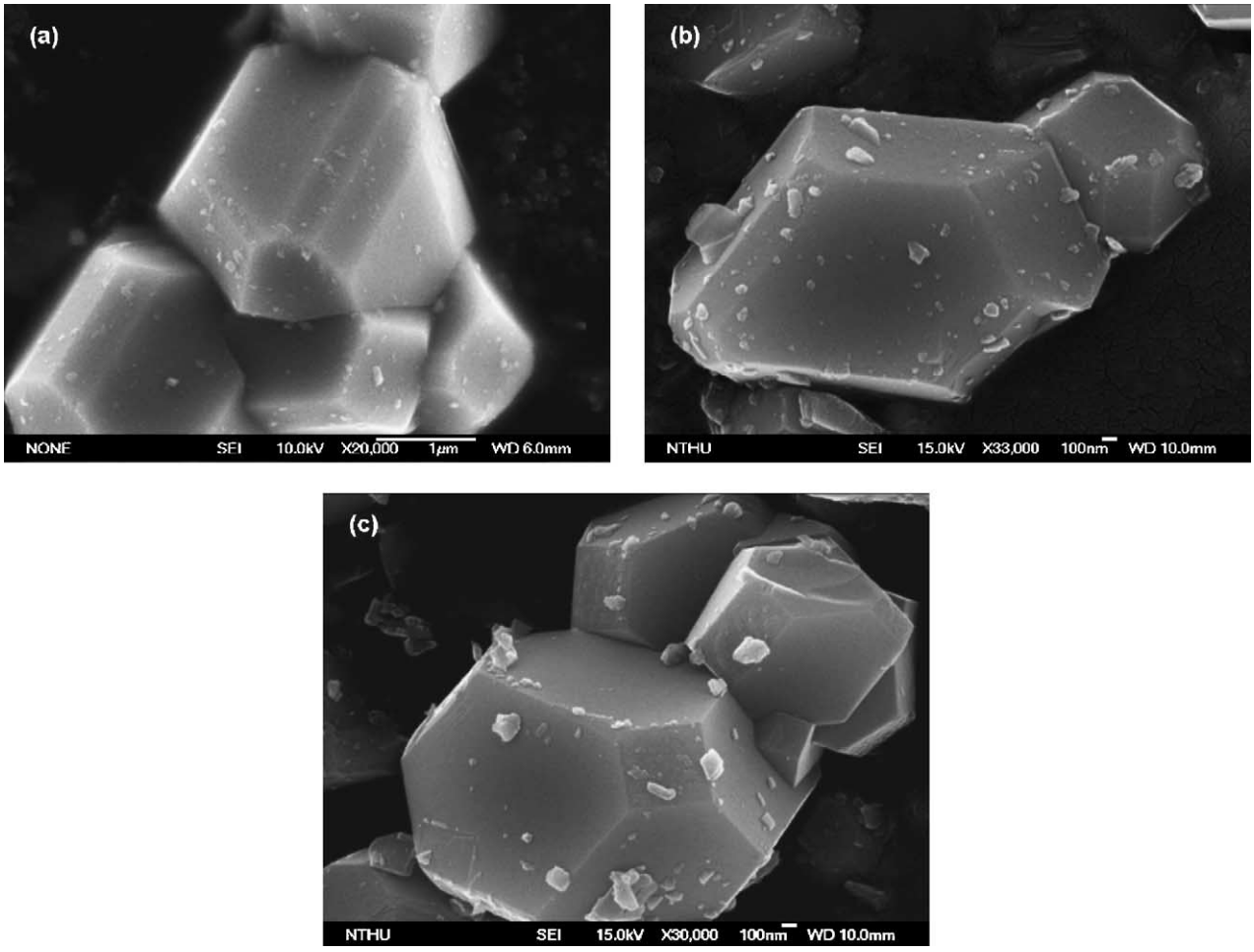

Fig. 7. FESEM images of various powders calcined at 870 °C for 15 h: (a) $LiMn_2O_4$; (b) $Li_{1.08}Mn_2O_4$; (c) $Li_{1.1}Mn_2O_4$.

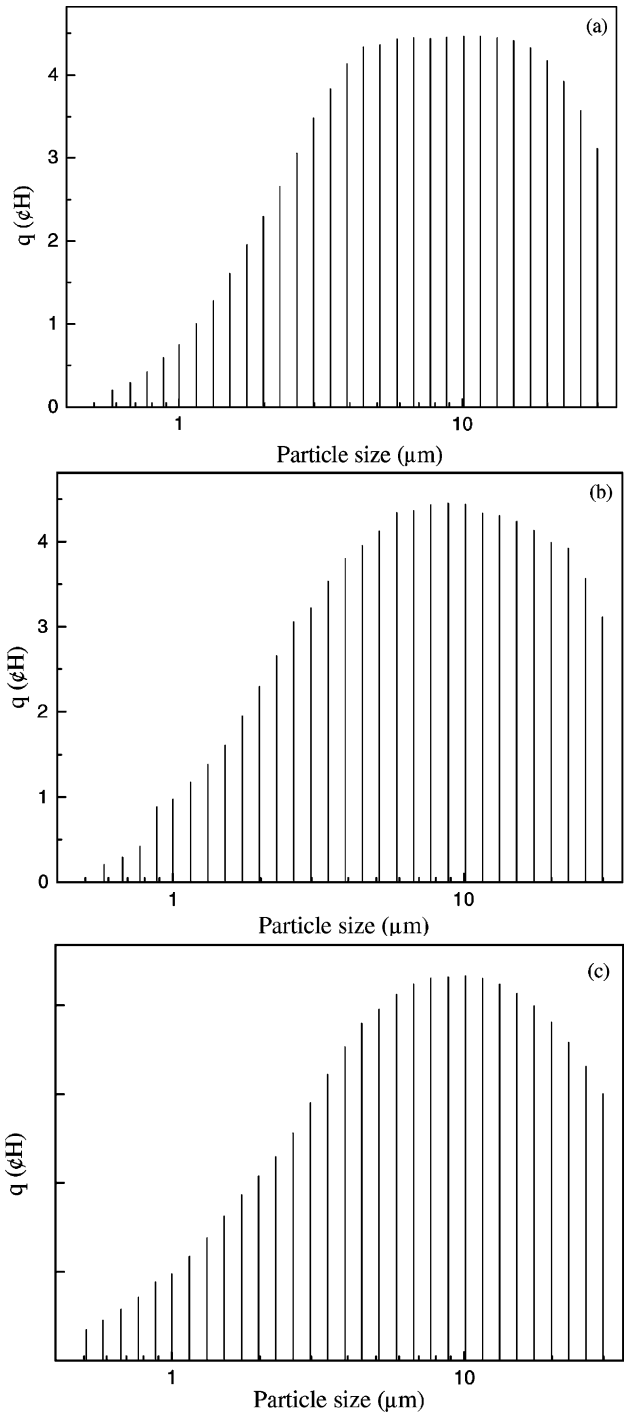

Fig. 8. Particle-size distribution of various powders calcined at 870 °C for 15 h: (a) $LiMn_2O_4$; (b) $Li_{1.08}Mn_2O_4$; (c) $Li_{1.1}Mn_2O_4$.

Precursors with nominal $LiMn_2O_4$ and Li excess $Li_{1+x}Mn_2O_4$ were sintered at various temperatures for different periods. Detailed phase identifications for powders sintered under various conditions have been carried out and are summarized in Table 2. It is concluded that pure spinel phase is obtained for powders sintered at high temperature for long periods. For powders sintered for only 5 h at a temperature below 800 °C, an impurity phase of Mn_2O_3 is observed. Nearly all the Mn_2O_3 disappears, however, if sintering is conducted for more than 10 h.

It should be noted that powders sintered as low as 700 °C for more than 10 h also exhibit a pure spinel phase, as indicated in Table 2. A larger particle size in the range 5–10 μm is required to assemble a Li-ion battery for practical applications. Thus, powders sintered at higher temperature, such as those shown in the upper right section of Table 2, are more suitable for battery assembly.

The data in Fig. 4b show that the XRD peaks shift towards higher diffraction angles. This is attributed to a small change in the crystal structure. There is also an implication of the fact that a trace amount of the excess Li^+ ions has been indeed been doped into the cubic spinel structure.

On the basis of the XRD results, the lattice constant of calcined powder was evaluated by a least-squares program, and then plotted against the calcined temperature, as indicated in Fig. 6. The lattice constant increases with temperature from 8.17 Å at 400 °C to 8.26 Å at 850 °C. This behavior suggests the gradual formation of stoichiometric spinel [12].

3.3. Particle size and morphology

Micrographs of sintered samples of $LiMn_2O_4$, $Li_{1.08}Mn_2O_4$ and $Li_{1.1}Mn_2O_4$ derived from the co-precipitation method and calcined at 870 °C for 15 h are shown in Fig. 7a–c, respectively. The morphology of Fig. 7a–c is corresponding to that of single-crystal with a cubic structure. The particles have a well-developed octahedral structure which is bounded by eight (1 1 1) planes [13].

The average particle size of $LiMn_2O_4$, $Li_{1.08}Mn_2O_4$ and $Li_{1.1}Mn_2O_4$ calcined at 870 °C for 15 h is 7.4, 8.1, and 8.3 μm, respectively, as shown in Fig. 8a–c. It appears that the particle size of $LiMn_2O_4$ is smaller than that of $Li_{1.08}Mn_2O_4$ and $Li_{1.1}Mn_2O_4$. The difference in particle size is considered to be due to the change of the valence of manganese that results from Li^+ doping. It is argued that excess lithium enhances the stability of the structure and allows more Li^+ ions to intercalate or de-intercalate through the cathode and the anode.

3.4. Electrochemical properties

The electrochemical behavior of lithium manganese oxide powders was also investigated. The first charge and discharge curves for $Li/Li_{1+x}Mn_2O_4$ coin cells ($x = 0$, 0.08 and 0.1) operated between 3 and 4.2 V are presented in Fig. 8. The first irreversible capacity of $LiMn_2O_4$ is 6 mAh g^{-1}, i.e. the difference between 90 mAh g^{-1} for first charge capacity and 84 mAh g^{-1} for first discharge capacity, as shown in Fig. 9a. $Li_{1.08}Mn_2O_4$ exhibits a value of 135 and 124 mAh g^{-1} for the charge and discharge capacities, respectively, and thus an irreversible capacity of 11 mAh g^{-1} is lost. Excess Li^+ ions in the $LiMn_2O_4$ powders leads to a considerably high

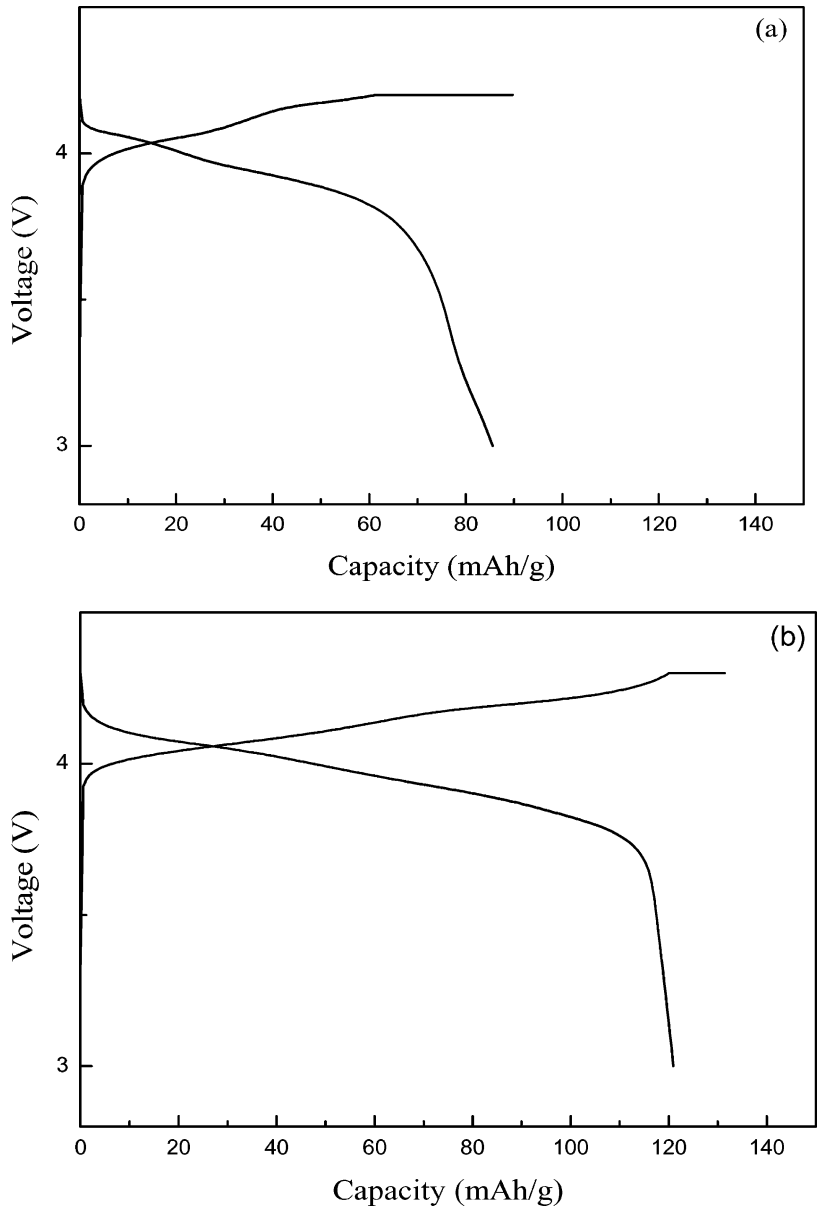

Fig. 9. First charge and discharge curves of various powders calcined at 870 °C for 15 h at the 0.1*C* rate (a) $LiMn_2O_4$ and (b) $Li_{1.08}Mn_2O_4$.

initial specific capacity and this partially compensates for the irreversible capacity loss.

The rate of capacity fading of $Li_{1+x}Mn_2O_4$ ($x = 0, 0.08$ and 0.1) was measured galvanostatically between 3 and 4.2 V for cells of configuration: $Li|EC + DMC + LiPF_6|Li_{1+x}Mn_2O_4$. The capacity of $LiMn_2O_4$ calcined at 870 °C for 15 h is 84.3 mAh g^{-1} for the first cycle but decays to 64.7 mAh g^{-1} after 16 cycles. The discharge capacity of $Li_{1.08}Mn_2O_4$ calcined at 870 °C for 15 h is 123.6 mAh g^{-1} for the initial cycle but retains 87% of its origin value after 16 cycles, which is a much better performance than that exhibited by $LiMn_2O_4$, as shown in Fig. 10. The larger decay in $LiMn_2O_4$ is due to the tail of the charge curve at 3.2 V and the plateau of the discharge curve between 4.1 and 4.2 V, which is caused by phase transformation during charging and discharging, as shown in Fig. 9a. The findings in this study demonstrate that cathode materials composed of excess Li spinel lithium manganese oxide and prepared by the co-precipitation method show relatively good stability and high specific capacity.

4. Conclusions

The following observations are made.

1. $Li_{1+x}Mn_2O_4$ powders doped with excess lithium are derived by the co-precipitation method with LiOH as the reactant, and sintered at temperatures between 400 and 870 °C for 5–15 h.

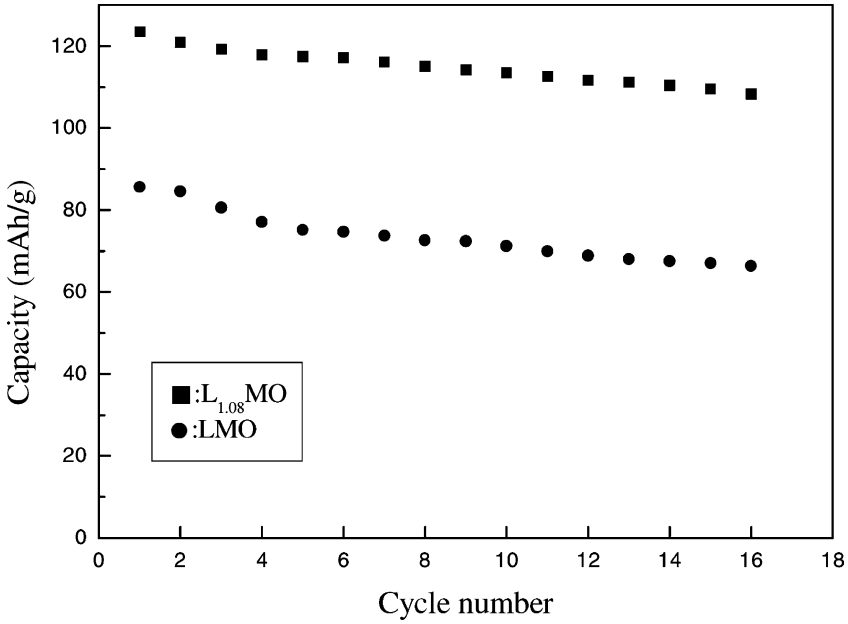

Fig. 10. Specific discharge capacities of $Li_{1+x}Mn_2O_4$ calcined at 870 °C for 15 h cycled at the 0.2*C* rate at room temperature.

2. With increase in sintering time and temperature, the initially formed Mn_2O_3 impurity is removed and a fully spinel structure is obtained.
3. The particle size of $LiMn_2O_4$ and excess Li doped $LiMn_2O_4$ calcined at 870 °C for 15 h is in the range 7–8 μm, which is very suitable for fabrication of coin cells.
4. Spinel $Li_{1+x}Mn_2O_4$ ($x = 0.08$ and 0.1) with uniform particle-size distribution shows good intercalation and de-intercalation performance and high initial capacity.

Acknowledgements

The first two authors are grateful to the Coremax Taiwan Corporation, Taiwan, for the financial support, with special thanks to the General Manager Mr. Jim Ho. The technical assistance by Mr. S.D. Wu in cell assembly is also appreciated. Partial support from National Science Council under the Contract No. NSC-90-2216-E007-070 is acknowledged.

References

[1] G.T.K. Fey, K.S. Wang, S.M. Yang, J. Power Sources 68 (1997) 159.
[2] D.G. Wickham, W.J. Croft, J. Phys. Chem. Sloids 7 (1958) 351.
[3] J.C. Hunter, J. Solid State Chem. 39 (1981) 142.
[4] M.M. Thackeray, W.I.F. David, P.G. Bruce, J.B. Goodenough, Mater. Res. Bull. 18 (1983) 461.
[5] R.T. Cygan, H.R. Westrich, D.H. Doughty, Mater. Res. Symp. Proc. 393 (1995) 113.
[6] J.M. Tarascan, F. Coowar, G. Amatuci, F.K. Shokoohi, D.G. Guyomard, J. Power Sources 54 (1995) 103.
[7] R. Manev, A. Momchilv, A. Nassalevska, A. Sato, J. Power Sources 54 (1995) 323.
[8] Q. Zhong, U. Sachen, J. Power Sources 54 (1995) 221.
[9] J.M. Tarascan, D.G. Guyomard, J. Electrochem. Soc. 138 (1991) 2864.
[10] R.J. Gummow, M.M. Thackeray, J. Electrochem. Soc. 141 (1994) 1178.
[11] R. Koksbang, J. Barker, H. Shi, M.Y. Saidi, Solid State Ionics 89 (1996) 1.
[12] A.R. Naghash, J.Y. Lee, J. Power Sources 85 (2000) 284.
[13] Y.K. Sun, B. Oh, H.J. Lee, Electrochim. Acta 46 (2001) 541.